Research Article

Journal of Chemistry Letters
journal homepage: www.jchemlett.com
ISSN (online): 2717-1892

A DFT study on the interaction of alprazolam with fullerene (C_{20})

Mohammad Reza Jalali Sarvestani [a, *], *Soma Majedi* [b]

[a] *Young Researchers and Elite Club, Yadegar-e-Imam Khomeini (RAH) Shahr-e-Rey Branch, Islamic Azad University, Tehran, Iran*

[b] *College of Health Sciences, University of Human Development, Sulaimaniyah, Kurdistan region of Iraq*

ARTICLE INFO

Article history:
Received 1 November 2019
Received in revised form 20 December 2019
Accepted 5 June 2020
Available online 5 June 2020

Keywords:
Alprazolam
Adsorption
Density functional theory
Fullerene
Detection

ABSTRACT

In this paper, the detection of alprazolam by fullerene (C_{20}) was studied by infrared (IR), frontier molecular orbital (FMO) and natural bond orbital (NBO) computations. All of the computations were done by density functional theory method in the B3LYP/6-31G (d) level of theory. The calculated adsorption energies, Gibbs free energy changes and thermodynamic constants showed alprazolam adsorption is experimentally possible, spontaneous and irreversible. The calculated values of enthalpy changes and specific heat capacity demonstrated alprazolam interaction with fullerene is exothermic and C_{20} can be used as a recognition element for the construction of a new thermal sensor for detection of alprazolam. The DOS spectrums showed the bandgap of fullerene decreased from 7.190 eV to 4.460 eV (%-37.9) in the alprazolam adsorption process and this nanostructure is a good electroactive sensing material for development of novel electrochemical sensors for alprazolam determination. Some important structural parameters including chemical hardness, chemical potential, electrophilicity, maximum charge capacity and the dipole moment of alprazolam in the adsorption process was also investigated.

1. Introduction

8-Chloro-1-methyl-6-phenyl-4H [1,2,4] triazolo [4,3-a] [1,4] benzodiazepine or alprazolam (AP, Figure 1) is a benzodiazepine prescribed for insomnia, depression, bipolar disorder, panic disorder and different kinds of phobia [1]. AP is one of the bestselling medicines and it is widely abused. Compressed tablets and extended-release capsules are the more commonly available forms of AP [2]. AP reacts selectively with the interaction sites of y-aminobutyric acid (GABA) receptors in the body and induces its effects by this mechanism [3]. The toxicity of AP is observable in high doses. Bradycardia, coma, nausea, diarrhea, syncope and even death are the common adverse effects of AP in high doses [4-7]. Therefore, developing a rapid, simple and sensitive thermal and electrochemical sensor for the detection of AP is very important [8].

On the other hand, in the fullerene family, C_{20} is the smallest member with a dodecahedral cage structure (Figure 1). C_{20} composed of pentagonal rings and its structure is highly curved. This nanostructure has special features that can make it an appropriate sensing material including high conductivity and outstanding reactivity and good surface area to volume ratio [9-11]. In this regard, the performance of this fullerene as an electrochemical and thermal sensing material for the detection of AP has been investigated for the first time in this research by density functional theory calculations.

* Corresponding author, e-mail: rezajalali93@yahoo.com

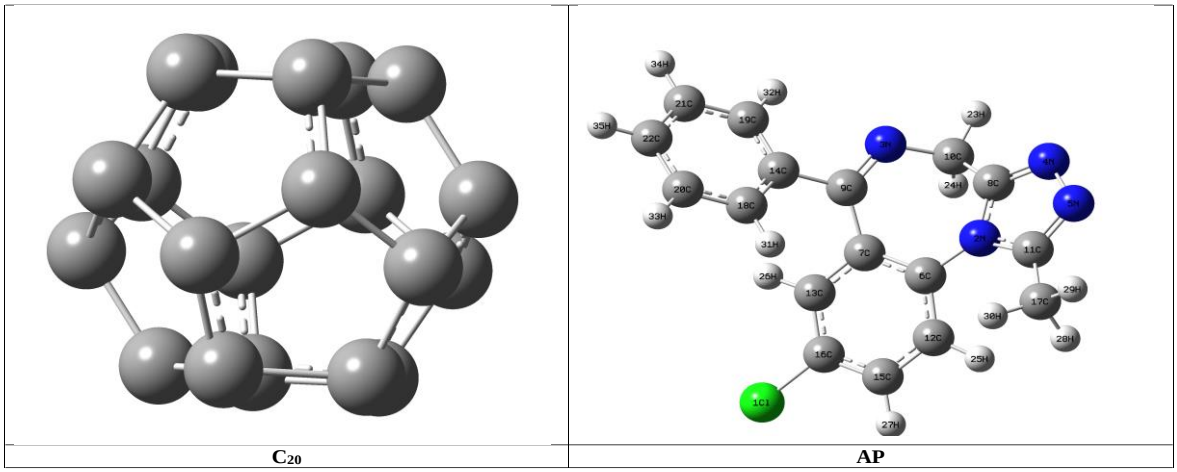

Figure 1. The optimized structures of C_{20} and AP

2. Results and discussion

Structural and NBO studies

As the provided initial and optimized structures in Figure 2 reveal clearly, the AP interaction with fullerene was scrutinized at two different modes. In I-Isomer the fullerene was inserted near the chlorine atom of AP but in II-Isomer, C_{20} was placed in parallel form near the diazepine ring of AP. As it is clear, at I-Isomer no obvious change can be distinguished in the structure of AP-C_{20} complex after geometrical optimization. However, at II-Isomer tangible deformation is seen after geometrical optimization in the structure of nanomaterial and the medicine molecule especially near the interacting site that can be due to the formation of chemical bonds between the adsorbent and the adsorbate [12]. In this respect, for obtaining more information about the adsorption mechanism the adsorption energies were calculated and NBO computations were performed on all of the structures and the results are presented in Table 1. According to Table 1, II-Isomer is more energetically stable than I-Isomer. Besides, the adsorption energy of II-Isomer (-275.600 kJ/mol) is more negative than the adsorption energy of I-Isomer (-95.107 kJ/mol) indicating the interaction is stronger in this position [13].

The NBO results that are also given in Table 1, indicates in I-Isomer no chemical bond was created between fullerene and AP. Therefore, the interaction in this mode is physisorption. While, in the case of II-Isomer, a monovalent bond with SP^3 hybridization and 1.620 (Å) bond length was created between C_{20} and one of the nitrogen atoms of triazolo ring of AP. Hence, the AP interaction with the nanostructure in this configuration is chemisorption [14].

The dipole moment of the structures was also calculated and the results are presented in Table 1. As can be seen, the dipole moment of AP is 4.14 but when it adsorbed on the surface of fullerene its dipole moment increased to 6.21 and 10.93 at I and II isomers respectively indicating the solubility of AP improves after its interaction with the nanostructure. The maximum (ν_{max}) and lowest vibrational frequencies (ν_{min}) of structures were also calculated by IR computations. As it is obvious from Table 1, no negative frequency was observed for the studied structures. Therefore, all of the investigated structures are in a true local minimum [15].

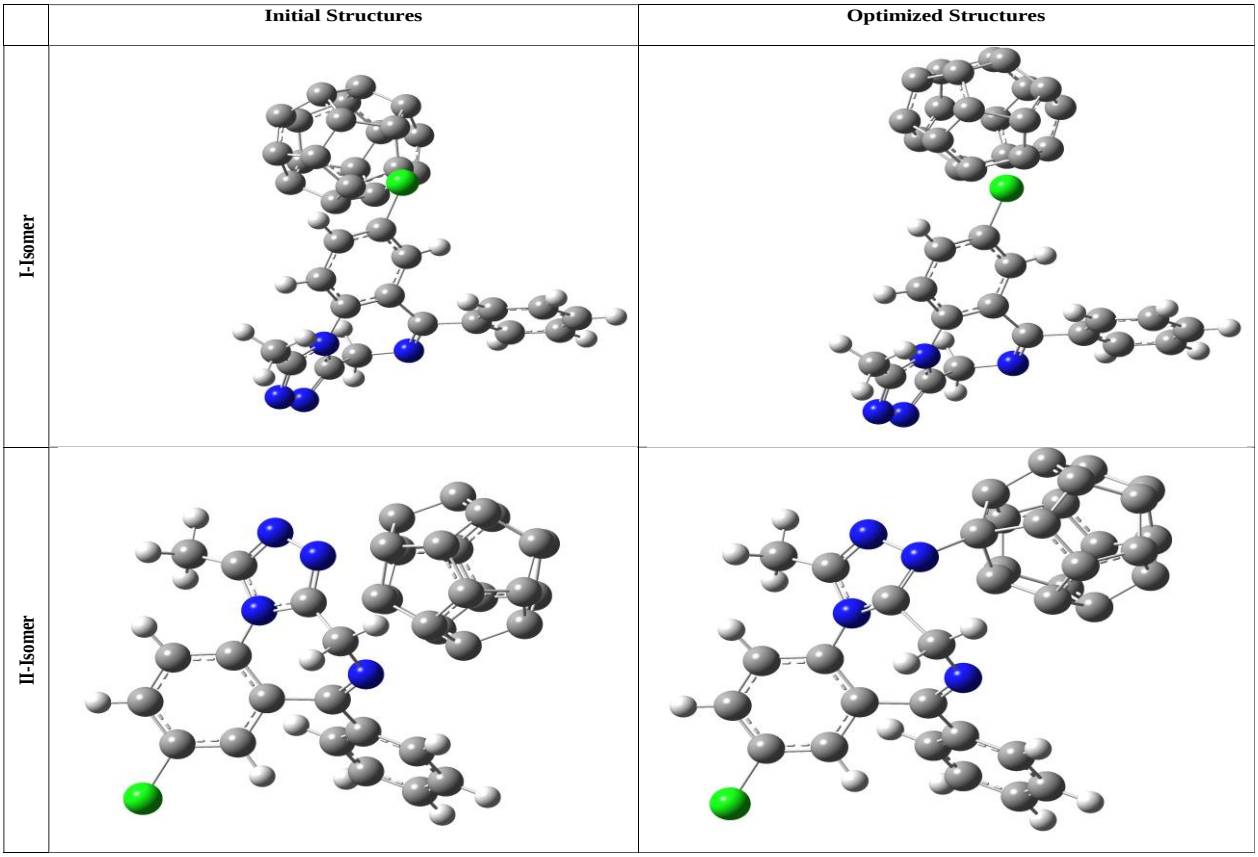

Figure 2. The initial and optimized structures of AP-C_{20} complexes

Table 1. The structural and NBO parameters of AP, C_{20} and their complexes

		Bond length (Å)	Bond order	Occupancy	Hybridization	Bond energy (a.u)	Total electronic energy (a.u)	Adsorption energy (kJ/mol)	ν_{min} (cm^{-1})	ν_{max} (cm^{-1})	Dipole Moment (Deby)
AP	---	---	---	---	---	---	-1312.976	---	39.469	3763.272	4.140
C_{20}	---	---	---	---	---	---	-747.196	---	261.392	1690.640	0.000
I-Isomer	---	---	---	---	---	---	-2060.235	-95.107	38.929	3763.506	6.210
II-Isomer	N-C	1.620	1.000	1.990	$SP^{2.98}$	-0.463	-2060.307	-275.600	28.703	3794.317	10.930

Thermodynamic parameters

The thermodynamic parameters of the adsorption process including enthalpy changes (ΔH_{ad}), Gibbs free energy changes (ΔG_{ad}), specific heat capacity (C_V) and the logarithm of thermodynamic equilibrium constant (Log K_{th}) were calculated in the temperature range of 298-398 K at 10˚ intervals and the results are presented in Figure 3. As it is clear, the ΔH_{ad} values for both configurations are considerably negative indicating the interaction is exothermic. Moreover, the specific heat capacity of fullerene increased remarkably when AP adsorbs on its surface which implies the thermal conductivity of nanostructure enhances in the AP adsorption process [16]. Hence, it can be deduced that C_{20} is a suitable sensing material for the construction of a new thermal sensor for AP detection. In these types of sensors, the desired analyte should have a highly exothermic or endothermic interaction with the recognition element that is immobilized on the surface of the sensor then, the carried out changes in the temperature of the sensor microenvironment will be detected by a sensitive thermistor and it will be used as a signal of measurement of the analyte. Owing to the exothermic nature of the adsorption process and enhancement of fullerene thermal conductivity it seems C_{20} is an appropriate sensing material for thermal detection of AP [17].

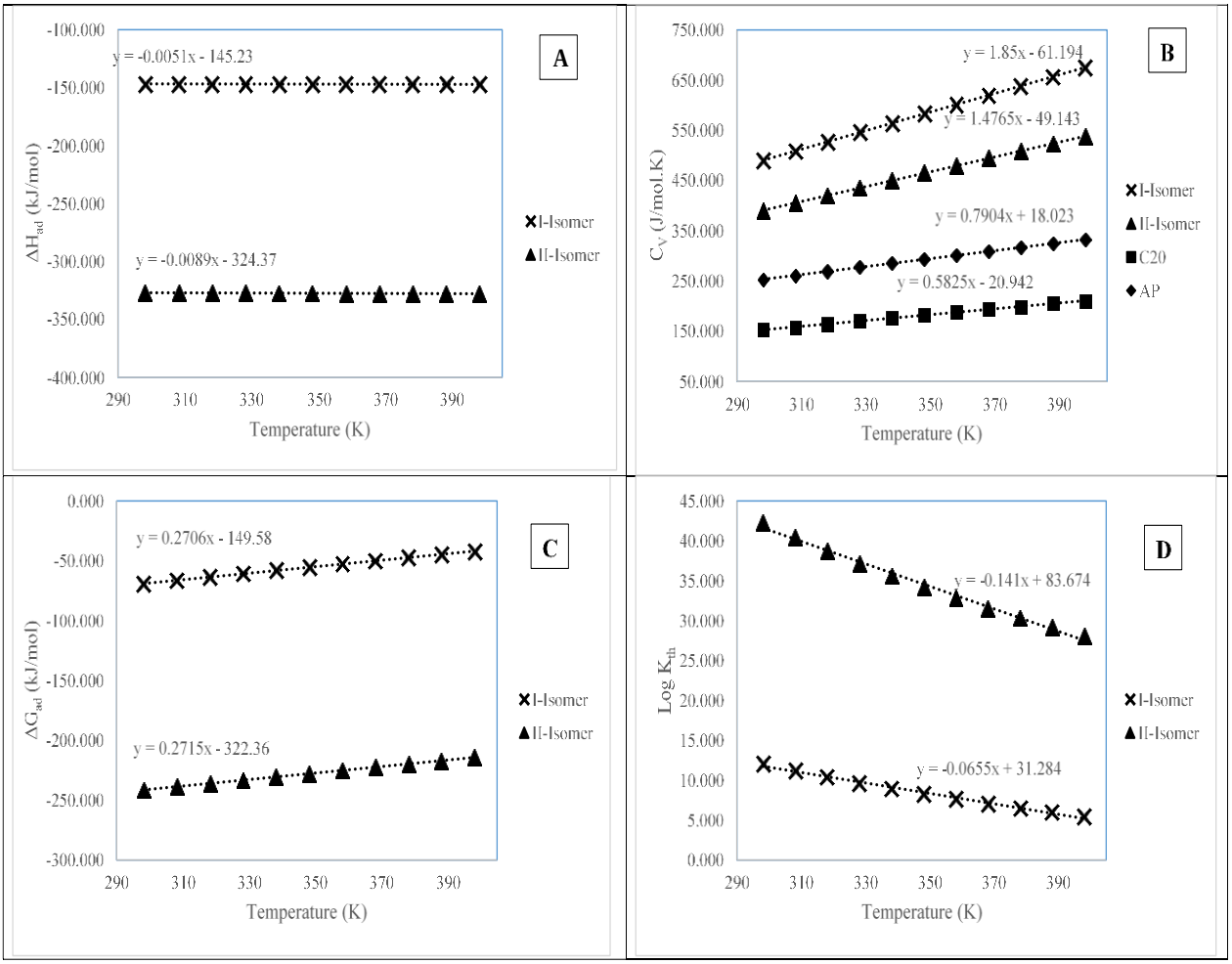

Figure 3. The values of ΔH_{ad} (A), C_V (B), ΔG_{ad} (C), Log K_{th} (D) in the temperature range of 298-398 K.

The calculated values of ΔG_{ad} and log K_{th} showed the AP interaction with fullerene is spontaneous and irreversible. The effect of temperature on the thermodynamic parameters was also checked out and the obtained results indicate the AP adsorption is more favorable in lower temperatures [18]. Indeed, the values of ΔG_{ad} and log K_{th} experience a sharp increment and decrease respectively by temperature increasing.

FMO analysis

The discrepancy of the highest occupied molecular orbital (HOMO) and the lowest unoccupied molecular orbital (LUMO) is defined as bandgap (Eg) in chemistry. This parameter has an inverse relationship with the electrical conductivity of molecules. In fact, the molecules with low bandgaps are more conductive than compounds with wide bandgaps [19]. In this respect, for investigating the performance of C_{20} as an electroactive sensing material for the development of a novel electrochemical sensor for AP detection, the DOS spectrums and bandgap of the studied structures were calculated and the results are presented in Figure 4. As it is clear, the bandgap of fullerene (7.190 eV) decreases about -27.344% in the case of I-Isomer to 5.224 eV and -37.968% in the case of II-Isomer to 4.460 eV [9-11]. Therefore, it can be concluded that the electrical conductivity of C_{20} improves substantially when AP adsorbs on its surface and this nanomaterial can be used for designing new electrochemical sensors for AP determination [12].

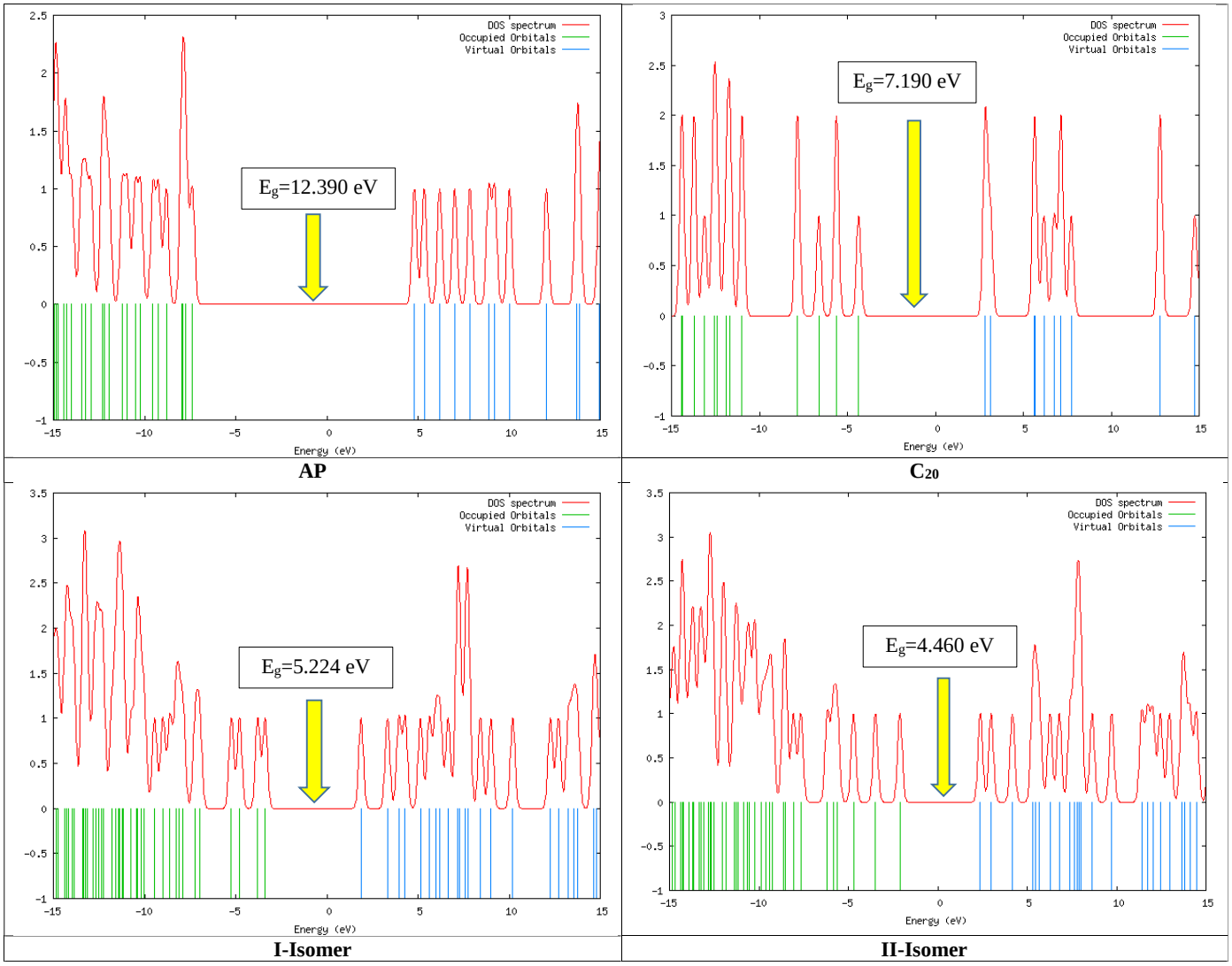

Figure 4. The DOS spectrums of AP, C_{20} and their complexes

The chemical hardness (η) and chemical potential (μ) of the studied structures were also evaluated and the results are given in Table 2. Both parameters are appropriate standards for estimating the reactivity of molecules. In other words, the compounds with lower chemical hardness and higher chemical potential values will be more reactive because necessary electron transmissions for implementation of a chemical reaction can be done in them more conveniently [13]. As can be observed, when AP adsorbs on the surfaces of C_{20} η decreases and μ increases tangibly in both configurations indicating the reactivity of AP enhances after its adsorption on the surface of fullerene.

Electrophilicity (ω) and maximum charge capacity (ΔN_{max}) were the last investigated parameters. As the obtained results in Table 2 show obviously when AP adsorbs on the surface of the adsorbent ω declines remarkably in both isomers which implies the affinity of AP decreases when it adsorbs on the surface of the nanostructure [14].

Table 2. The frontier molecular orbital parameters of AP, C_{20} and their complexes

	E_{HOMO}	E_{LUMO}	Eg	$\%\Delta E_g$	η	μ	ω	ΔN max
AP	-7.520	4.870	12.390	---	6.195	-1.325	0.142	0.214
C_{20}	-4.350	2.840	7.190	---	3.595	-0.755	0.079	0.210
I-Isomer	-3.361	1.863	5.224	-27.344	2.612	-0.749	0.107	0.287
II-Isomer	-2.097	2.363	4.460	-37.968	2.230	0.133	0.004	-0.060

3. Computational Details

The structures of Fullerene, AP and their complexes were designed by Nanotube modeler 1.3.0.3 and GuassView 6 softwares [20, 21]. At the first step, the designed structures were optimized geometrically. Then, IR, NBO and FMO computations were implemented on them. All of the computations were performed by Gaussian 16 software by the density functional theory method in the B3LYP/6-31G (d) level of theory because in former studies about nanomaterials its results were in a good agreement with the experimental data [22]. The density of states (DOS) spectrums was obtained by GuassSum 3.0 software [23]. All of the calculations were implemented in the aqueous medium and in the temperature range of 298-398 at 10˚ intervals.

The studied processes were as follows:

$$\text{AP} + \text{Fullerene} \longrightarrow \text{AP-Fullerene} \quad (1)$$

The values of adsorption energy values (E_{ad}) and thermodynamic parameters including adsorption enthalpy changes (ΔH_{ad}), Gibbs free energy changes (ΔG_{ad}) and thermodynamic equilibrium constants (K_{th}) were calculated by Equations 2-5 respectively.

$$E_{ad} = \left(E_{(\text{AP-Fullerene})} - \left(E_{(\text{AP})} + E_{(\text{Fullerene})} + E_{(\text{BSSE})}\right)\right) \quad (2)$$

$$\Delta H_{ad} = \left(H_{(\text{AP-Fullerene})} - \left(H_{(\text{AP})} + H_{(\text{Fullerene})}\right)\right) \quad (3)$$

$$\Delta G_{ad} = \left(G_{(\text{AP-Fullerene})} - \left(G_{(\text{AP})} + G_{(\text{Fullerene})}\right)\right) \quad (4)$$

$$K_{th} = \exp\left(-\frac{\Delta G_{ad}}{RT}\right) \quad (5)$$

In the referred equations, E is the total electronic energy of each structure, E_{BSSE} denotes the basis set superposition correction energy, H stands for enthalpy of the evaluated materials. The G denotes Gibbs free energy, R is the ideal gas constants, T denotes the temperature [9-11].

Frontier molecular orbital parameters including bandgap (E_g), chemical hardness (η), chemical potential (μ), electrophilicity (ω) and the maximum charge capacity (ΔN_{max}) were calculated by equations 6-10 [32].

$$\text{Eg} = E_{LUMO} - E_{HOMO} \quad (6)$$

$$\%\Delta Eg = \left(\frac{Eg2 - Eg1}{Eg1}\right) \times 100 \quad (7)$$

$$\eta = {}^{(E_{LUMO} - E_{HOMO})}/_{2} \quad (8)$$

$$\mu = {}^{(E_{LUMO} + E_{HOMO})}/_{2} \quad (9)$$

$$\omega = {}^{\mu^2}/_{2\eta} \quad (10)$$

$$\Delta N_{max} = -{}^{\mu}/_{\eta} \quad (11)$$

E_{LUMO} and E_{HOMO} in equations 6 to 11 are the energy of the lowest unoccupied molecular orbital and the energy of the highest occupied molecular orbital respectively. The Eg1 and Eg2 in Equation 7, are the bandgap of AP-C_{20} complex and bandgap of C_{20} respectively [12-14].

4. Conclusion

AP is a benzodiazepine type medicine that is abused widely. In this respect, its detection is of great importance. For this reason, the performance of C_{20} as a sensing material for thermal and electrochemical detection of AP was evaluated by density functional theory calculations in this study for the first time. The calculated values of adsorption enthalpy changes and specific heat capacity showed AP adsorption on the surface of fullerene is exothermic and this nanomaterial is an excellent sensing material for the development of a new thermal sensor for AP determination. The influence of temperature on the AP adsorption process studied and the findings indicated the interaction process is more favorable in lower temperatures. The DOS spectrums showed the bandgap of C_{20} declined %-37.9 in its interaction process with AP and as a consequence, it can be used for the fabrication of new electrochemical sensors for AP measurement.

Acknowledgements

The authors appreciate the young researchers and elite club of Islamic Azad University of Yadegar-e-Imam Khomeini (RAH) Shahre-rey branch for supporting this project.

References

1. P. Samiec, Z. Navratilova, Electrochemical behaviour of bromazepam and alprazolam and their determination in the pharmaceutical tablets Lexaurin and Xanax on carbon paste electrode. Monatsh. Chem., 148 (2017) 449-455.
2. Y. Panahi, A. Motaharian, M. R. Milani Hosseini, O. Mehrpour, High sensitive and selective nano-molecularly imprinted polymer based electrochemical sensor for midazolam drug detection in pharmaceutical formulation and human urine

samples, Sens. Actuat. B. Chem., 273 (2018) 1579-1586.
3. M. R. Ganjali, H. Haji-Hashemi, F. Faridbod, P. Norouzi, Potentiometric Determination of Alprazolam based on Carbon Paste and PVC membrane Electrodes, Pharmaceutical Formulation and Human Serum. Int. J. Electrochem. Sci., 7 (2012) 1470 – 1481.
4. H J. Narang, N. Malhotra, C. Singhal, A. Mathur, A. Krishna PN, C. S. Pundir, Detection of alprazolam with a lab on paper economical device integrated with urchin like Ag@ Pd shell nano-hybrids. Mater. Sci. Eng. C., 80 (2017) 728-735.
5. N. L. Fincur, J. B. Krstic, F. S. Šibul, D. V. Šojic ´, V. N. Despotovic, N. D. Banic, J. R. Agbaba, B. F. Abramovic, Removal of alprazolam from aqueous solutions by heterogeneous photocatalysis: Influencing factors, intermediates, and products. Chem. Eng. J., 307 (2017) 1105–1115.
6. U. K. Chhalotiya, N. M. Patel, D. A. Shah Falgun A. Mehta, K. K. Bhatt, Thin-layer chromatography method for the simultaneous quantification and stability testing of alprazolam and mebeverine in their combined pharmaceutical dosage form. J. Taibah. Univ. Sci., 11 (2017) 66-75.
7. S. Akram, S. N. Ali, A. Qayoom, S. Iqbal, N. Naz, I. Memon, High Performance Liquid Chromatographic Method for Simultaneous Determination of Alprazolam with Antihistamines in Bulk Drug, Pharmaceutical Formulation and Human Serum. Sindh. Univ. Res. Jour., 49 (2017) 07-12.
8. P. Samiec, Ľ. Švorc, D. M. Stanković, M.Vojs, M. Marton, Z. Navrátilová, Mercury-free and modification-free electroanalytical approach towards bromazepam and alprazolam sensing: A facile and efficient assay for their quantification in pharmaceuticals using boron-doped diamond electrodes. Sens. Actuat. B. Chem., 245 (2017) 963-971.
9. M. R. Jalali Sarvestani, R. Ahmadi, Investigating the Effect of Fullerene (C20) Substitution on the Structural and Energetic Properties of Tetryl by Density Functional Theory. J. Phys. Theor. Chem. IAU. Iran., 15 (2018) 15-25.
10. R. Ahmadi, M. R. Jalali Sarvestani, Adsorption of Tetranitrocarbazole on the Surface of Six Carbon-Based Nanostructures: A Density Functional Theory Investigation. Phys. Chem. B., 14 (2020) 198-208.

M. R. Jalali Sarvestani, R. Ahmadi, Adsorption of TNT on the surface of pristine and N-doped carbon nanocone: A theoretical study. Asian J. Nanosci. Mater., 3 (2020) 103-114.

11. M. R. Jalali Sarvestani, M. Gholizadeh Arashti, B. Mohasseb, Quetiapine Adsorption on the Surface of Boron Nitride Nanocage (B12N12): A Computational Study. Int. J. New. Chem., 7 (2020) 87-100.
12. M. R. Jalali Sarvestani, R. Ahmadi, Investigating the Complexation of a recently synthesized phenothiazine with Different Metals by Density Functional Theory. Int. J. New. Chem., 4 (2017) 101-110.
13. M. R. Jalali Sarvestani, R. Ahmadi, Adsorption of Tetryl on the Surface of B12N12: A Comprehensive DFT Study. Chem. Methodol., 4 (2020) 40-54.
14. S. Majedi, F. Behmagham, M. Vakili, Theoretical view on interaction between boron nitride nanostructures and some drugs. J. Chem. Lett., 1 (2020) 19-24.
15. H. G. Rauf, S. Majedi, E. A. Mahmood, M. Sofi, Adsorption behavior of the Al- and Ga-doped B12N12 nanocages on COn (n=1, 2) and HnX (n=2, 3 and X=O, N): A comparative study. Chem. Rev. Lett., 2 (2019) 140-150.
16. R. A. Mohamed, U. Adamu, U. Sani, S. A. Gideon, A. Yakub, Thermodynamics and kinetics of 1-fluoro-2-methoxypropane vs Bromine monoxide radical (BrO): A computational view. Chem. Rev. Lett., 2 (2019) 107-117.
17. S. Majedi, H. G. Rauf, M. Boustanbakhsh, DFT study on sensing possibility of the pristine and Al- and Ga-embeded B12N12 nanostructures toward hydrazine and hydrogen peroxide and their analogues. Chem. Rev. Lett., 2 (2019) 176-186.
18. R. Moladoust, Sensing performance of boron nitride nanosheets to a toxic gas cyanogen chloride: Computational exploring. Chem. Rev. Lett., 2 (2019) 151-156.
19. Nanotube Modeler J. Crystal. Soft., 2014 software.
20. GaussView, Version 6.1, R. Dennington, T. A. Keith, J. M. Millam, Semichem Inc., Shawnee Mission, KS, 2016.
21. Gaussian 16, Revision C.01, M. J. Frisch, G. W. Trucks, H. B. Schlegel, G. E. Scuseria, M. A. Robb, J. R. Cheeseman, G. Scalmani, V. Barone, G. A. Petersson, H. Nakatsuji, X. Li, M. Caricato, A. V. Marenich, J. Bloino, B. G. Janesko, R. Gomperts, B. Mennucci, H. P. Hratchian, J. V. Ortiz, A. F. Izmaylov, J. L. Sonnenberg, D. Williams-Young, F. Ding, F. Lipparini, F. Egidi, J. Goings, B. Peng, A. Petrone, T. Henderson, D. Ranasinghe, V. G. Zakrzewski, J. Gao, N. Rega, G. Zheng, W. Liang, M. Hada, M. Ehara, K. Toyota, R. Fukuda, J. Hasegawa, M. Ishida, T. Nakajima, Y. Honda, O. Kitao, H. Nakai, T. Vreven, K. Throssell, J. A. Montgomery, Jr., J. E. Peralta, F. Ogliaro, M. J. Bearpark, J. J. Heyd, E. N. Brothers, K. N. Kudin, V. N. Staroverov, T. A. Keith, R. Kobayashi, J. Normand, K. Raghavachari, A. P. Rendell, J. C. Burant, S. S. Iyengar, J. Tomasi, M. Cossi, J. M. Millam, M. Klene, C. Adamo, R. Cammi, J. W. Ochterski, R. L. Martin, K. Morokuma, O. Farkas, J. B. Foresman, and D. J. Fox, Gaussian, Inc., Wallingford CT, 2016.
22. N. M. O'Boyle, A. L. Tenderholt, K. M. Langner, A Library for Package-Independent Computational Chemistry Algorithms. J. Comp. Chem., 29 (2008) 839-845.